

ESI: Coarse-grained molecular simulations of the melting kinetics of small unilamellar vesicles

Lara A. Patel,^{*a} and James T. Kindt^a

1 Truncated icosahedron assembly

It is possible to calculate internal dihedral angles between faces that share an edge for a truncated icosahedron through application of geometric identities and the constraints that:

1. Every vertex of a truncated icosahedron is the product of an intersection of a pentagonal face and two hexagonal faces.
2. The length of all pentagon and hexagon edges are equal.
3. The edge length l_{edge} is directly correlated to the distance, r_{face} , between the center of the truncated icosahedron and any face on the shape.

The results of this can be seen in Sections ?? and ??.

The displacement of the lipid slabs if they were a two-dimensional surface is given by Equation ?? for a given edge length l_{edge} . The slabs however occupy a three-dimensional space and their displacement must account for the thickness of the bilayer l_{thick} (~ 4 nm). If we assume that the distance r_{face} is defined as the distance to the center of mass of the pentagonal or hexagonal slab, a good first approximation to the appropriate slab displacement is given by Equation ?. In practice, we generated a series of truncated icosahedron with different displacements, chose the displacement that provided sufficient overlap of lipids in both leaflets at edges. That configuration was then subjected to a script that identifies lipid pairs that have a minimum separation less than 0.45 nm and removes one of the lipids.

$$r_{\text{face}}(l_{\text{edge}}) = l_{\text{edge}} \left(\frac{9}{2} \sqrt{\frac{17+6\sqrt{5}}{109}} \right) \quad (\text{S1})$$

$$r_{\text{slab}}(l_{\text{edge}}) = r_{\text{face}}(l_{\text{edge}}) + l_{\text{thick}}/2 \quad (\text{S2})$$

1.1 Hexagonal faces

The dihedral angle between a pentagon face and a neighboring hexagon face θ_{ph} is 37.4° (Equation ??) and the dihedral angle between two hexagon faces θ_{hh} is 41.8° (Equation ??).

$$\theta_{\text{ph}} = \frac{180}{\pi} \left(\pi - \sin^{-1} \left[\frac{2\sqrt{65-22\sqrt{5}}}{15-3\sqrt{5}} \right] - \sin^{-1} \left[\frac{3+\sqrt{5}}{6} \right] \right) \quad (\text{S3})$$

$$\theta_{\text{hh}} = \frac{180}{\pi} \left(\pi - 2 \sin^{-1} \left[\sqrt{\frac{3+\sqrt{5}}{6}} \right] \right) \quad (\text{S4})$$

$$\theta_{\text{rot}} = \frac{2\pi}{5} \left(\frac{180}{\pi} \right) \quad (\text{S5})$$

Starting with a hexagonal slab, Fig. ?? shows that a strip of the truncated icosahedron hexagons can be constructed by rotating a hexagonal slab displaced from the origin by a distance r_{slab} by the angles θ_{ph} and θ_{hh} . Rotating the whole strip by the angle θ_{rot} of 72.0° about a \hat{C}_5 rotational axis of the truncated icosahedron four times gives rise to the hexagon-only structure in the center of the top row of Fig. ??.*

^a Emory University, Chemistry Department, 1515 Dickey Drive, Atlanta, GA 30322, USA. Tel: +1 404 712 2983; E-mail: lapatel@emory.edu; E-mail: jkindt@emory.edu

*A variation of this structure with 12 intentional pores (the pentagonal faces) to serve as defect sinks was used in early calculations but the resulting structure was slow to close.

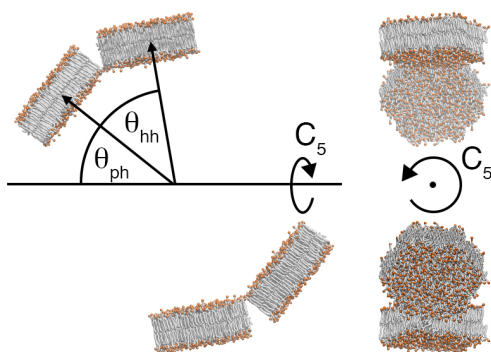


Fig. S1 The diagram above illustrates the relevant angles used in the construction of a strip of four hexagonal slabs. The angle between two hexagonal faces θ_{hh} and the angle between a hexagonal and pentagonal face θ_{ph} are marked on the right side image relative to a \hat{C}_5 rotational axis. Four subsequent rotations of the strip around that axis are then used to place the rest of the hexagons as shown in the left side image of Fig. ??.

1.2 Pentagonal faces

The angle between two pentagons separated by the edge of two intersecting hexagons θ_{pp} is 62.2° (Equation ??).

The first pentagonal slab of lipids is displaced from the origin by a distance r_{slab} . The next pentagon is generated by rotating the first by 36.0° about the radial vector that goes from the origin of the truncated icosahedron to the middle of the pentagon slab (the \hat{C}_5 rotational axis) and then rotating by θ_{pp} towards the \hat{C}_2 rotational axis which is marked in Fig. ?. This pentagon is then subsequently rotated about the \hat{C}_5 rotational axis by θ_{rot} four more times so that the hemisphere in Fig. ?? is the result. This structure is then rotate by 180.0° around the axis perpendicular to the \hat{C}_2 and \hat{C}_5 axes to get the pentagon-only structure seen in the first image in the first row of Fig. ??

$$\theta_{pp} = \frac{180}{\pi} \left(\cos^{-1} \left[\frac{36419 + 5296\sqrt{5}}{52369} \right] + 2 \cos^{-1} \left[\frac{-9(55 + 13\sqrt{5})}{-5 + \sqrt{5}} \sqrt{\frac{5 - \sqrt{5}}{122149 + 49863\sqrt{5}}} \right] \right) \quad (S6)$$

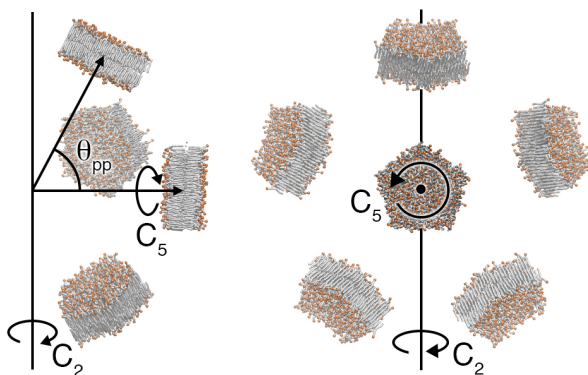


Fig. S2 The diagram illustrates the the relevant angles used in the construction of the first half of the pentagons used to construct a truncated icosahedron. This half is constructed by first rotating the middle pentagon out towards the \hat{C}_2 axis by θ_{pp} . This pentagon is then rotated around the central pentagon by θ_{rot} . The half of the pentagons is then rotated around the \hat{C}_2 by 180.0° .

The pentagon-only truncated icosahedron (Fig. ??, left) and hexagon-only truncated icosahedron (Fig. ??, center) are combined (Fig. ??, right), and a bad contact distance of 0.45 nm is implemented. Any pair of lipid within 0.45 nm of one another are flagged and one of the lipids is removed. The result of the combination and effect of removing bad contacts can be seen in the bottom row of snapshot in Fig. ??.

2 Supplementary Figures

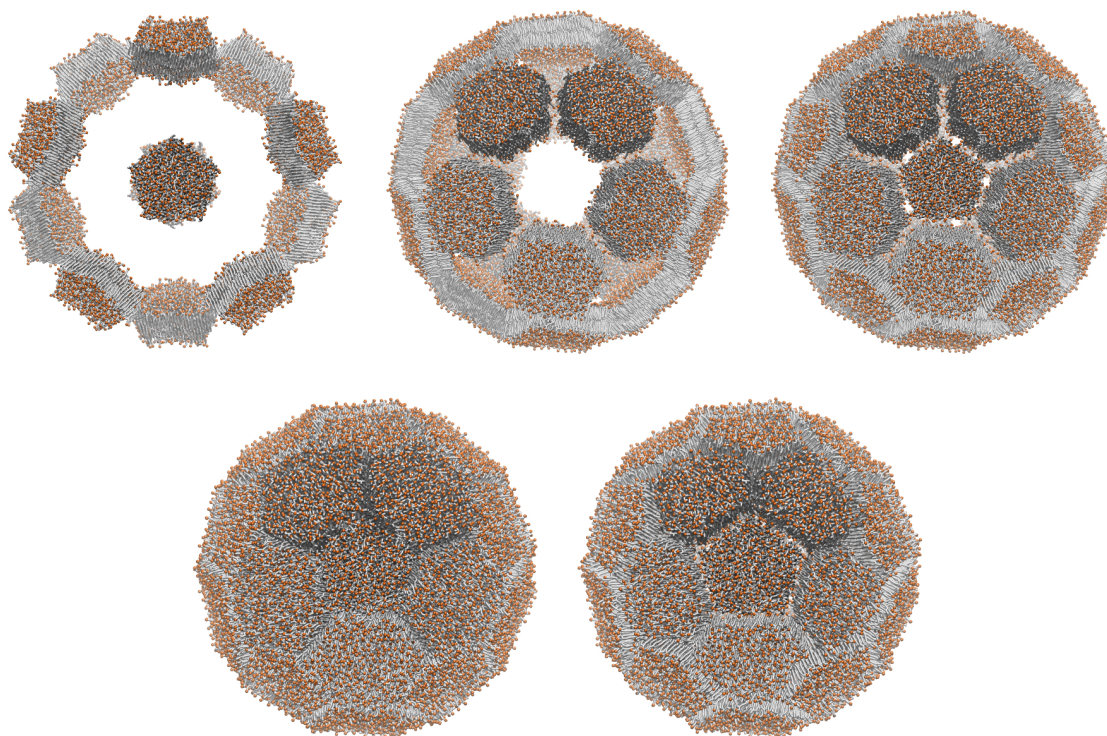


Fig. S3 The first row of images are a 'blown up' schematic of the vesicle assembly. From right to left we have the pentagonal faces of a truncated icosahedron constructed from gel phase slabs of DPPC lipids, the hexagonal faces of a truncated icosahedron constructed likewise from gel phase DPPC lipids, and the result of concatenating the two sets of lipids to form the full truncated icosahedron. The second row shows what happens when a shorter displacement is used. The first vesicle is one with bad contacts between lipids and the second is the same vesicle after lipids within 0.45 nm of another lipid have been removed.

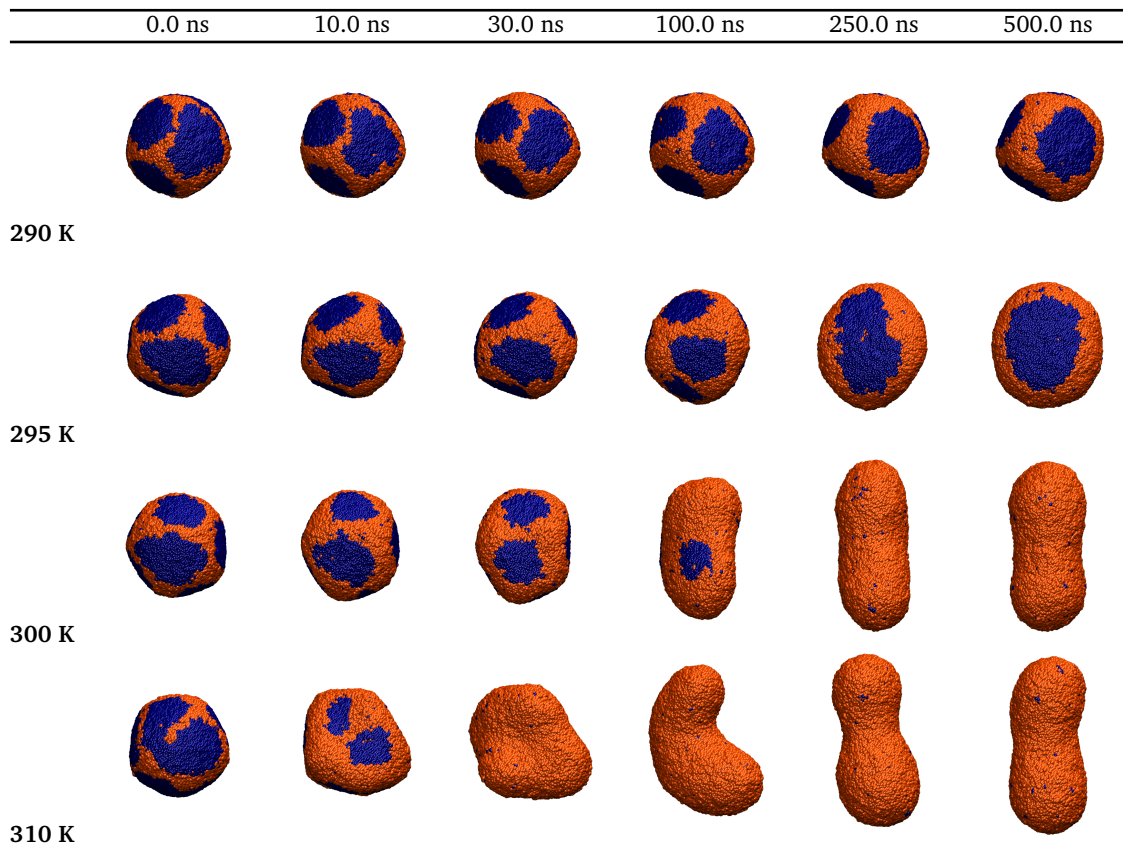


Fig. S4 Melting progression for the 33 nm vesicle melting at 290 K, 295 K, 300 K and 310 K.

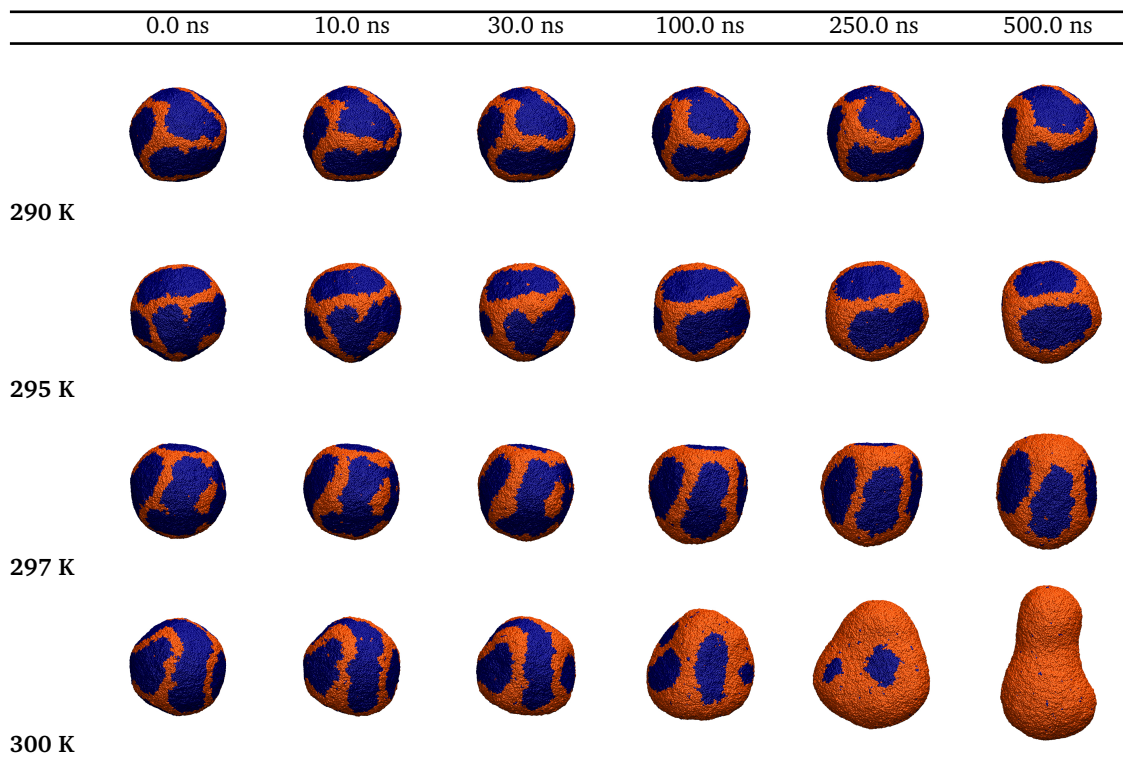


Fig. S5 Melting progression for the 50 nm vesicle at 290 K, 295 K, 297 K, and 300 K.

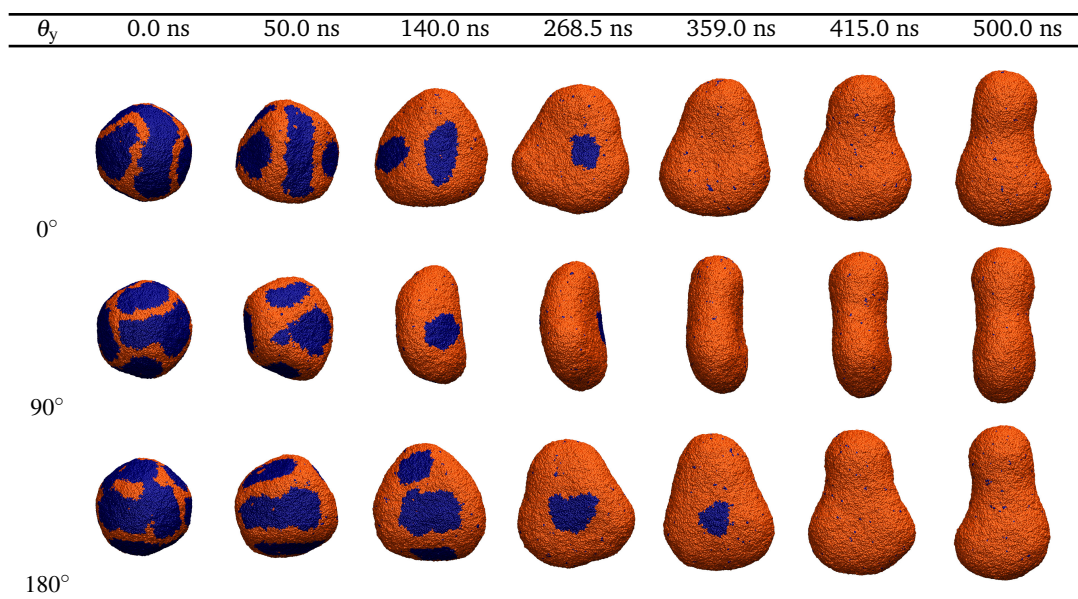


Fig. S6 Shape of the 50 nm melting at 300 K over a 500 ns trajectory. The rows show the vesicle rotated about the vertical axis of the vesicle by 90°.

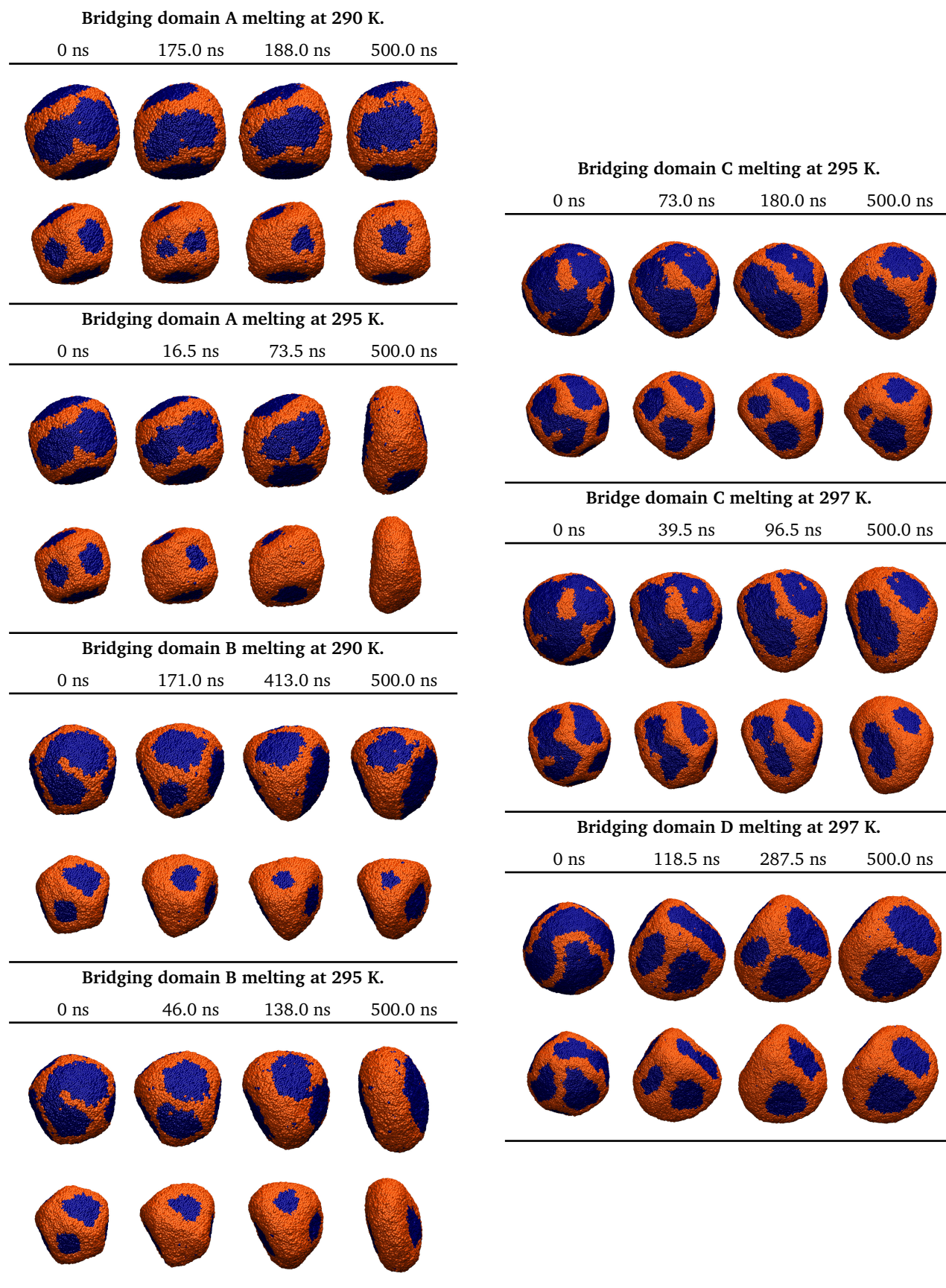
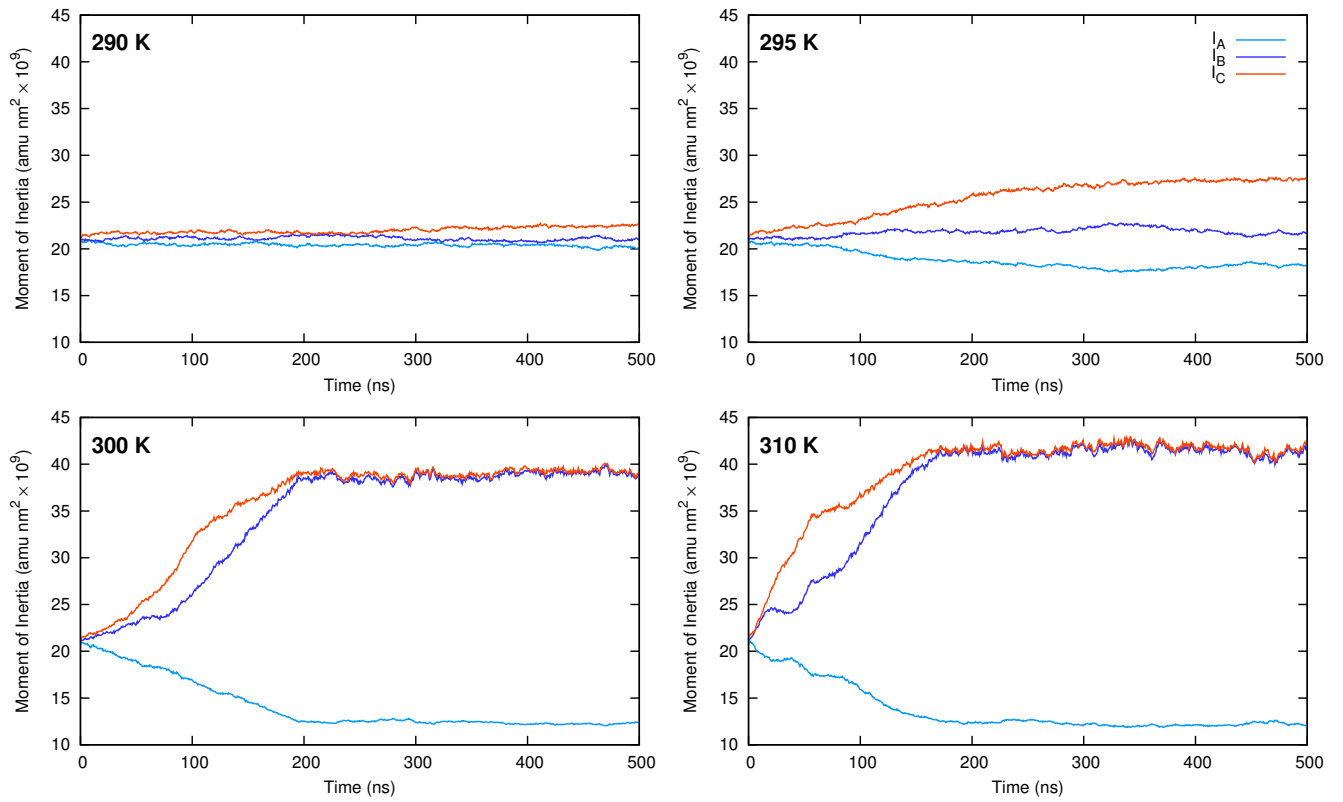


Fig. S7 Snapshots of bridging domains melting in the inner and outer leaflets of vesicles with diameters of 33 nm (right) and 50 nm (left).

A



B

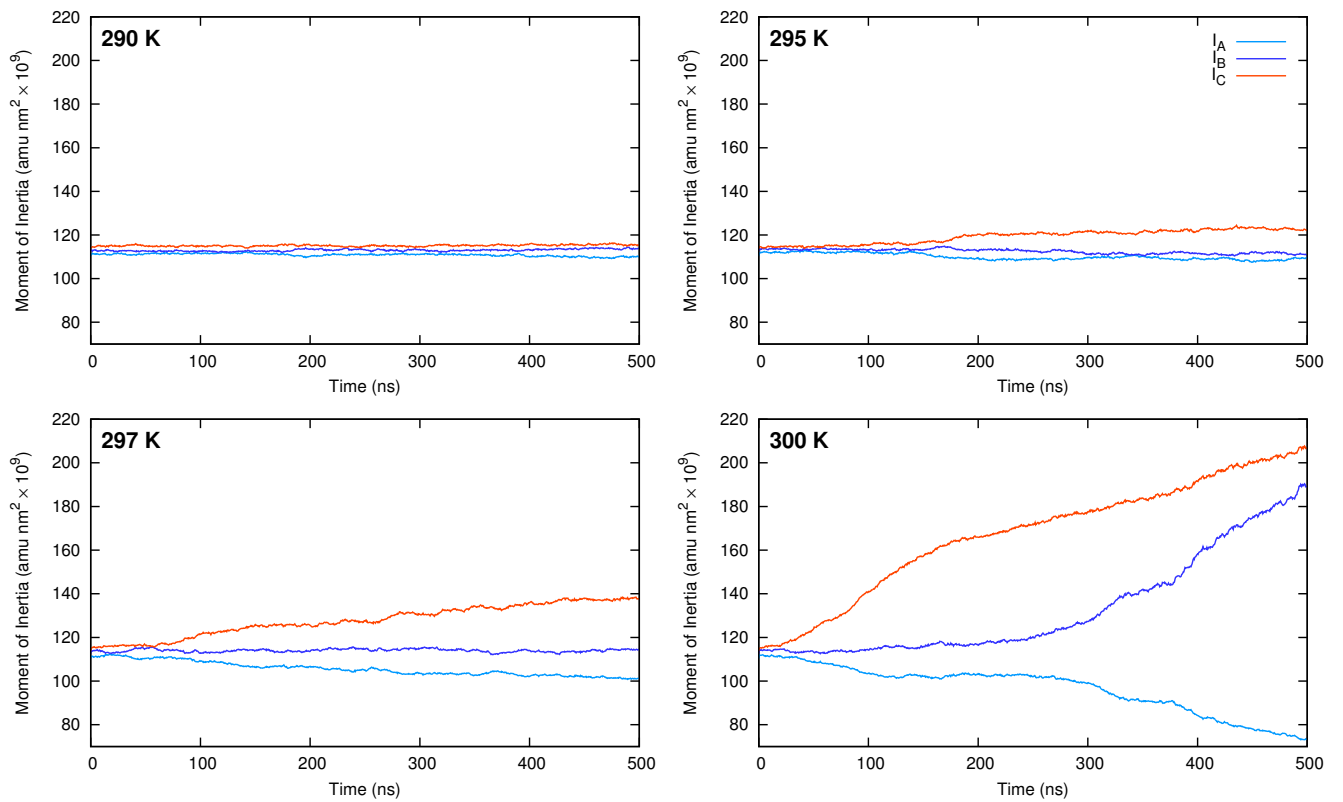


Fig. S8 Plots of the primary moments of inertial for the 33 nm vesicle (A) and the 50 nm vesicle (B) over the 500 ns trajectory of melting. The moments of inertial are arranged such that $I_A \leq I_B \leq I_C$. Partial melting occurs for the 33 nm vesicle at 290 and 295 K with full melting to a prolate symmetry at 300 and 310 K. Partial melting for the 50 nm vesicle occurs at 290, 295, and 297 K and complete melting at 300 K to end with a pear shape.